minerals

MDPI

Article

Proposed Methodology to Evaluate CO_2 Capture Using Construction and Demolition Waste

Domingo Martín [1], Vicente Flores-Alés [2] and Patricia Aparicio [1,*]

[1] Departamento de Cristalografía, Mineralogía y Q. Agrícola, Facultad de Química, Universidad de Sevilla, 41012 Sevilla, Spain; dmartin5@us.es

[2] Departamento de Construcciones Arquitectónicas II, Escuela Técnica Superior de Ingeniería de Edificación, Universidad de Sevilla, 41012 Sevilla, Spain; vflores@us.es

* Correspondence: paparicio@us.es

Received: 8 August 2019; Accepted: 1 October 2019; Published: 5 October 2019

Abstract: Since the Industrial Revolution, levels of CO_2 in the atmosphere have been constantly growing, producing an increase in the average global temperature. One of the options for Carbon Capture and Storage is mineral carbonation. The results of this process of fixing are the safest in the long term, but the main obstacle for mineral carbonation is the ability to do it economically in terms of both money and energy cost. The present study outlines a methodological sequence to evaluate the possibility for the carbonation of ceramic construction waste (brick, concrete, tiles) under surface conditions for a short period of time. The proposed methodology includes a pre-selection of samples using the characterization of chemical and mineralogical conditions and in situ carbonation. The second part of the methodology is the carbonation tests in samples selected at 10 and 1 bar of pressure. The relative humidity during the reaction was 20 wt %, and the reaction time ranged from 24 h to 30 days. To show the effectiveness of the proposed methodology, Ca-rich bricks were used, which are rich in silicates of calcium or magnesium. The results of this study showed that calcite formation is associated with the partial destruction of Ca silicates, and that carbonation was proportional to reaction time. The calculated capture efficiency was proportional to the reaction time, whereas carbonation did not seem to significantly depend on particle size in the studied conditions. The studies obtained at a low pressure for the total sample were very similar to those obtained for finer fractions at 10 bars. Presented results highlight the utility of the proposed methodology.

Keywords: suitable methodology for mineral carbonation; construction and demolition waste

1. Introduction

CO_2 emissions into the atmosphere are a growing environmental problem in different industrial sectors. The construction sector is no stranger to this problem considering gaseous emissions are derived from manufacturing processes of materials used mostly in construction, such as ceramic materials or cement [1]. Independent of the existing controversy regarding the uncertainty of the sensitivity of the climate in the international scientific community [2], the most negative forecasts consider some of the effects predicted by the uncontrolled emission of greenhouse gases as a possible increase in Earth's temperature, climatic alterations that will accelerate desertification, and a possible loss of part of the coastline due to the rise in sea levels.

In the current scenario, the challenges of reducing emissions cannot solely be met with greater energy efficiency and renewable energy resources in the generation phase. It is absolutely necessary to act on the management and treatment of emissions. For this reason, research aimed at capturing CO_2 is of vital importance in order to achieve the standards set as an objective.

Mineral-carbonation systems for CO_2 fixation are another option for Carbon Capture and Storage (CCS). Although less efficient than geological storage, they are much simpler, cheaper, and have fewer requirements, which responds to the requirement of ecological rationality raised above. The present work deals with the possibilities of using construction and demolition waste as CO_2 reservoirs. Preliminary research has shown that construction materials containing calcium and/or magnesium in their composition in the form of silicates, oxides, and hydroxides, which can react with CO_2 to give rise to carbonates, thus constituting a possible alternative for mineral carbonation from ceramic waste within options for CO_2 capture/storage [3–6]. This possibility is based on the capacity of construction and demolition waste with a high content of calcium and/or magnesium in the form of silicates, oxides, and hydroxides to fix CO_2 under optimal conditions, using a chemical reaction whose product is the formation of carbonates and silica as stable by-products. This process of carbonation occurs naturally with very slow kinetics; it is of interest to design a system and methodology to accelerate this process to make the capture of CO_2 from anthropogenic activity profitable, achieving maximal industrial and energy efficiency. There are several patents and studies that use residues with a high calcium content from different types of industrial waste for their carbonation [7–22].

The present work presents a methodological sequence for the control and validation of a viable alternative of CCS using mineral carbonation of construction and demolition waste (bricks, concrete, tiles) with a high content of silicates rich in calcium and magnesium. In this case, those with a high content of ceramic materials and cementitious conglomerate (mortar and concrete) can be considered optimal landfills for their transformation into CO_2 sinks [23,24].

A laboratory model was tested that indicated the efficiency of the system, ensuring extrapolated conditions at a landfill scale were in accordance with the difficulty involved in the reproduction of parameters that can be controlled at a laboratory scale. In this sense, it is necessary to establish a system that approximately reproduces conditions of isolation, humidity, dimensions, and others that, with generic character, can be reached in a controlled residue deposit. The physical–chemical and mineralogical mechanisms, the external conditions that have a decisive influence on the process, and the kinetics of capture and carbonation reactions that favor gas fixation and stabilization were analyzed. The control and verification procedures of the process were also analyzed, which allowed the adequate monitoring and optimization of the process.

2. Materials and Methods

2.1. Materials and Carbonation Test

The material used for the development of this methodology proposal was a brick type widely used in construction, which was specifically a clinker brick (MPC2) from Malpesa S.L. (Bailén, South of Spain) fired at 1050 °C.

The samples were subjected to a crushing process for granulometric conditioning. Fractions of less than 4 mm were selected to obtain size ratios consistent with the diameter of the reactor, obtaining homogeneous distribution so that there was a predominance of coarser fractions corresponding to conventional waste shredding.

Carbonation tests were carried out in a 0.3 L volume hermetic reactor (Parr Instruments Co., Moline, IL, USA). The fixed conditions were 10 bars of CO_2, 4:1 solid–water ratio, and room temperature. The variable conditions were reaction time (between 24 and 720 h) and particle size (<4, 2–4, and 1–2 mm). These particle-size fractions were selected because they were the most representative results of the crushing treatment. Additionally, a test was carried at low pressure (1 bar), room temperature, and a 4:1 solid–water ratio in a 5 L volume hermetic reactor of continuous flow to maintain pressure at 1 bar during the 720 h of reaction time.

Post-treatment, the samples were dried at 100 °C for 24 h, powdered, and sieved at 50 μm for subsequent analysis.

2.2. Instrumental Techniques: Methodology

Major multielemental chemical composition (in oxides) was performed with an automated Panalytical Axios model wavelength-dispersive X-ray fluorescence spectrometer (WDXRF). The samples were prepared for analysis as glass discs to reduce the "matrix effect."

The mineralogical composition of the untreated and treated samples was determined by X-ray diffraction (XRD) using a Bruker D8 Advance diffractometer (Bruker AXS, Berlin, Germany) with standard monochromatic Cu–Kα radiation at 40 kV and 30 mA with a Ni filter and Linxeye 1D detector. Routine scanning was performed with a 0.015° 2θ step size, and at 0.1 s per step from 3° to 70°. Rietveld refinement was also realized to determine the quantitative composition of the untreated bricks. In this case, scanning was performed with a 0.010° 2θ step size at 0.5 s per step in the range of 3°–120° and adding zincite (15 wt %) as an internal standard. Rietveld refinement for the present phase quantification was done with Bruker's commercial Topas v5 software (Bruker AXS, Berlin, Germany).

In addition, previous carbonation analysis was carried out by X-ray diffraction using a Bruker D8 Advance powder diffractometer (Bruker AXS, Berlin, Germany) equipped with an Anton Paar XRK 900 reactor chamber (Anton Parr GmbH, Graz, Austria) and high-sensitivity detector Bruker Vantec 1 (Bruker AXS, Berlin, Germany). This chamber was designed for X-ray diffraction experiments of up to 900 °C and 10 bar for solid state–gas reactions. Standard monochromatic Cu–Kα radiation operating at 40 kV and 40 mA was employed. Scanning was performed with a 0.022° 2θ step size at 0.2 s per step from 3° to 70°. Samples were in a CO_2-rich environment for 24 h in this reactor chamber.

Macro- and micro-observations were obtained by stereomicroscope using a Greenough Leica S8 APO (Leica Microsystems GmbH, Wetzlar, Germany) equipped with a DC300 camera (Leica Microsystems GmbH, Wetzlar, Germany) and by scanning electronic microscopy (SEM) using a JEOL 6460 LV microscope (JEOL Ltd., Akishima, Japan) equipped with energy-dispersive spectrometers (Oxford Instruments INCA, Oxford, UK).

The carbonate content of the carbonated samples was determined by two analytical methods: differential thermal and thermogravimetric analysis (DTA-TG) and an elemental analyzer. DTA-TG were performed on a TG Netzsch STA 409 PC. Samples (around 150 mg) were heated in an aluminum oxide crucible under a nitrogen atmosphere at 10 °C min^{-1} from room temperature to 1200 °C. Weight loss was measured by thermogravimetric analysis in the temperature range of 450–900 °C relative to the total carbonated decomposition. Elemental carbon content was measured using an elemental analyzer, Leco Truspec CHNS Micro (St. Joseph, MI, USA), which calculated the carbonated ratio by assuming that the whole carbon content was calcite.

Soluble Si, Ca, and Mg ions of the original and treated samples were also determined. Analysis was performed with simultaneous inductively coupled plasma optical emission spectrometry (IPC-OES) analysis using a Horiba Jobin Yvon ULTIMA 2 model instrument (Horiba Scientific, Palaiseau, France). The samples were prepared by mixing the solid-powder samples with water and stirring for 24 h, isolating the liquid phase by centrifugation, and filtering using a Nylon 0.22 μm syringe filter (MilliporeSigma, Burlington, MA, USA).

Specific surface area (BET) and microporosity were measured with a Micromeritics Gemini 2360 instrument (Micromeritics Instrument Corp, Norcross, GA, USA) using the absorption of N_2 at liquid nitrogen temperature. Before measuring, all samples were degassed using a Flow Prep 060 Micromeritics degasser (Micromeritics Instrument Corp, Norcross, GA, USA) with dry nitrogen gas at 80 °C for 12 h. Nanoporosity was measured with an ASAP 2420 instrument (Micromeritics Instrument Corp, Norcross, GA, USA) using CO_2 absorption at room temperature. Samples were degassed at 150 °C for 1.5 h and finally outgassed to 10^{-3} Torr. Macro- and mesoporosity were studied using mercury porosimeter Quantachrome Instruments Pore Master 60-GT (Quantachrome Instruments, Boynton Beach, FL, USA).

3. Results and Discussion

3.1. Proposed Methodological Sequence to Evaluate Effectiveness of Construction and Demolition Waste for CCS

A first outcome measure to take into consideration to provide the optimal construction residue is to have an important content of calcium oxide and/or magnesium as reactive compounds, since these elements are necessary for precipitation in the form of the carbonate, although the carbonation of other alkali metals is possible, as shown in the following equations [25]:

$$MO + CO_2 \rightarrow MCO_3. \quad (1)$$

This reaction is usually exothermic in nature, as per Lackner et al. (1995) [26]:

$$CaO + CO_2 \rightarrow CaCO_3 + 179 \text{ kJ/mole} \quad (2)$$

$$MgO + CO_2 \rightarrow MgCO_3 + 118 \text{ kJ/mole}. \quad (3)$$

Consequently, sample characterization requires a chemical analysis that is commonly used (WDXRF).

It has been widely described in the literature that the main possible carbonation minerals are oxides, silicates, and anhydrite; therefore, it was necessary to determine the minerals present in the sample in order to evaluate the candidate. Natural wollastonite is a widely studied mineral in several works, for example, Huijgen and coworkers [27], as a candidate for mineral carbonation. Different studies used other types of sample, such as industrial waste, that were mainly composed of wollastonite [28–30].

The proposed methodology includes a sample preselection using the characterization of chemical and mineralogical conditions, and in situ carbonation. The second part of the methodology is carbonation tests in the selected samples. The flow diagram of the proposed methodology is shown in Figure 1.

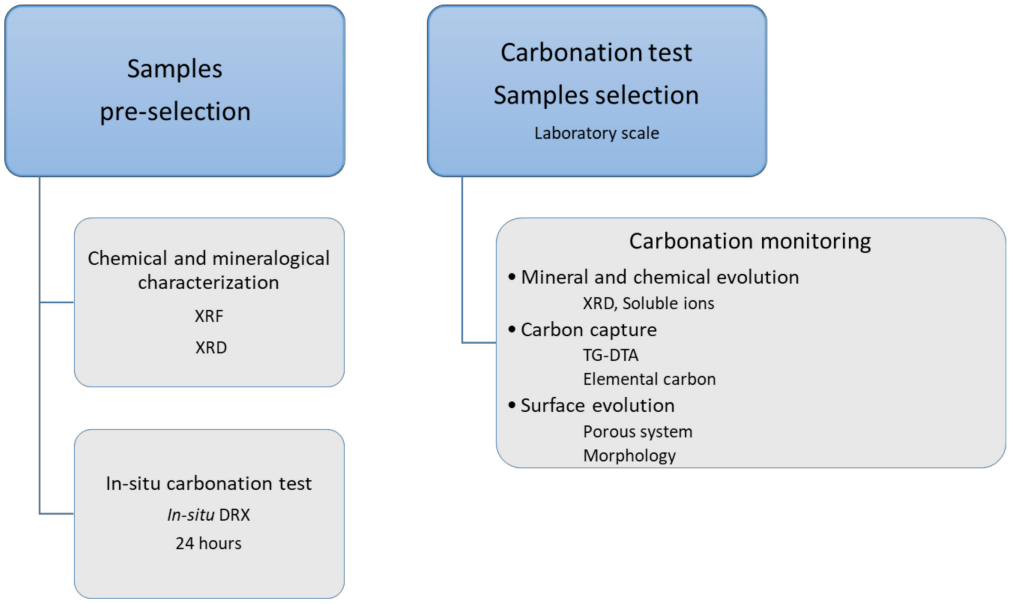

Figure 1. Flow diagram of proposed methodology.

For that reason, mineral characterization by powder X-ray diffraction is commonly used. In the same way, we propose an in situ carbonation test and process the evaluation by using a diffractometer equipped with a reaction chamber in a CO_2-rich environment. We mixed 2 g of the powdered sample and a couple of pipetted drops, and took a scan every six hours over the course of 24 h. These tests

made it possible to obtain the first analysis of carbonation evolution, selecting a feasible candidate for the carbonation tests.

Once the carbonation tests were completed, the treated samples had to be analyzed by XRD, showing the presence of carbonate phases as carbonation by-products. Rietveld refinement of both the treated and the original sample allowed the quantification of the present phases, determining the percentage of new stable carbonate phases and the destruction (or partial destruction) of phases that provided the necessary calcium and/or magnesium.

Likewise, the presence of new precipitated minerals could be observed by SEM. Combined with microchemical composition from energy-dispersive spectrometers (EDS), it confirmed the possible by-product phase. If the precipitate was large enough, then the optical microscopy supply provided information on how the precipitate grew on the surface of the sample and texture, as well as estimating sizes.

As an alternative to the quantification processes, and especially when these new phases did not represent a sufficient percentage for correct quantification, to quantify the amount of CO_2 capture, two techniques were employed: elemental carbon measure and weight loss by differential thermal and thermogravimetric analysis (DTA-TG) in the temperature range of carbonate mineral decomposition. In the first case, CO_2 capture can be calculated by the direct conversion of carbon to dioxide (CO_2 (wt %) = 3.6641 × C (wt %)) for the difference of the carbon content in the original and the treated sample. In the second one, weight-loss measuring in the right temperature range corresponding to the thermal decomposition of carbonates for the difference between treated and the original sample corresponded to the percentage by weight of captured CO_2. Since it was different, if any of the minerals constituting the samples had total or partial decomposition in the same temperature range, they would not be quantified, since they would be present in both samples pre- and post-treatment, for example, carbonates that already originally existed. The evolution of soluble ion content helps what follows mineral destruction.

Another aspect to take into consideration was the evaluation of the specific surface area by Brunauer–Emmett–Teller (BET) analysis. This technique can help us understand how the specific surface of a sample evolves at the microscopic level (the texture). Complete porosity analysis from the nano- to the macroscale also allows a study of the porous system after carbonation by isotherm adsorption of CO_2 and N_2. In this sense, it was possible to analyze how the precipitate completed the sample-surface pores, reducing their size to a smaller scale from the macro- or mesoscale to the micro- or nanoscale.

Finally, it is common in the literature to use the Steinour formula [21,24,31–33] to determine the efficiency of the reaction from the theoretical maximal CO_2 sequestration value obtained from the following stoichiometric formula (Equation (4)):

$$CO_2(\text{wt \%}) = 0.785(\%CaO - 0.7\%SO_3) + 1.09\%MgO + 0.71\%Na_2O + 0.468\%K_2O. \quad (4)$$

3.2. Validation of Proposed Methodology Using Ca-Silicate-Rich Brick

For each of the techniques described in the previous section, an example of the obtained results for the selected sample for this study (MPC2) and the correlations between them is presented. However, this example sample was already studied in more detail in a previous work of some of the authors in mineral carbonation processes [5].

In the MPC2 sample, CaO was around 15 wt % and 2 wt % for MgO (Table 1 and Tables S1–S3 in Supplementary Materials), which were appropriate values to be considered candidates for the mineral-carbonation process. This sample was composed of quartz, k- and alkali feldspar, plagioclases (orthoclase, anorthite, and albite), and calcium-rich silicate as wollastonite (Figure 2 and Table 2).

Table 1. Chemical composition of original brick MPC2 (wt %) by X-ray fluorescence (XRF) (modified from [5]).

Sample	SiO_2	Al_2O_3	Fe_2O_3	MnO	MgO	CaO	Na_2O	K_2O	TiO_2	P_2O_5	SO_3	LOI	TOTAL
MPC2	56.8	16.6	5.4	0.1	1.9	14.8	0.6	2.6	0.9	0.1	0.3	0.8	100.8
Detection Limit (DL)	0.01	0.01	0.01	0.02	0.01	0.04	0.01	0.02	0.03	0.01	0.22		
Quantification Limit (QL)	0.02	0.02	0.02	0.03	0.02	0.05	0.03	0.03	0.10	0.02	0.23		
Relative Error	0.012	0.020	0.058	0.184	0.007	0.047	0.038	0.028	0.061	0.025	0.063		

LOI: loss on ignition at 1025 °C.

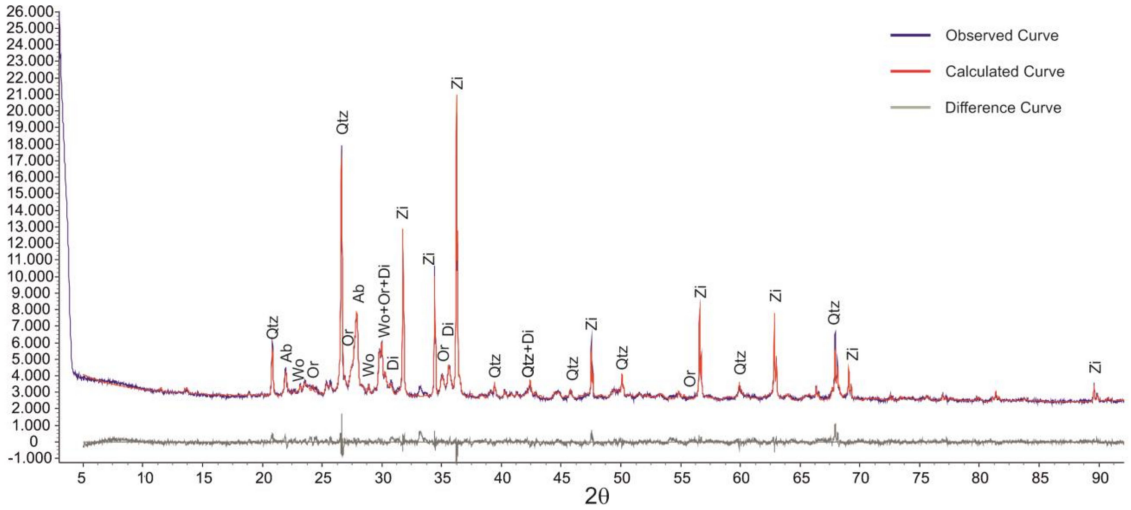

Figure 2. X-ray diffraction (XRD) pattern of MPC2 (and Rietveld refinement). Abbrv.: Qtz—quartz; Ab—Albite; Wo—wollastonite; Or—orthoclase; Di—diopside; Zi—zincite (Internal Standard).

Table 2. Mineralogical composition (wt %) of selected brick MPC2 (Qtz: quartz; Wo: wollastonite; Or: orthoclase; Ab: albite; Di: diopside; An: anorthite; Amor: amorphous phase). Rexp, Rwp, and GOF are numerical indicators of how well the Rietveld model was refined. Rwp, residual of least-squares refinement (weighted), which must be improved in refinement (with common sense); Rexp evaluates data quality; and GOF, goodness of fit parameter.

Sample	Qtz	Wo	Or	Ab	Di	An	Amor
MPC2	20.5	6.2	3.7	11.8	4.7	29.5	23.6
Rietveld Refinement	Rexp:	1.86	GOF:	1.72	Rwp:	3.21	

An in situ carbonation test (Figure 3) showed the evolution of newly grown calcite over time in a CO_2-rich environment. Intensity for the main calcite's peak (at d = 3.04 Å) increased directly proportional to time.

The next step was to perform carbonation tests on a laboratory scale with the selected bricks according to previous analysis, the high content of CaO, mineralogical composition rich in Ca silicate, and the presence of calcite in the in situ carbonation test. Tests were performed at room temperature and 10 bar pressure for different reaction times, and three fractions of particle sizes were representative of the total. Additionally, a test was carried out for the original sample at low pressure (1 bar), room temperature, and a 4:1 solid–water ratio in a 5 L volume hermetic reactor for 720 h of reaction time.

In the X-ray patterns of treated samples, compared with the nontreated, the most obvious differences were the presence of calcite, and the partial destruction of wollastonite and some orthoclase. The attack on wollastonite with carbonic acid allowed for the release of calcium ions and calcite precipitation [4–6,27,28,34–36].

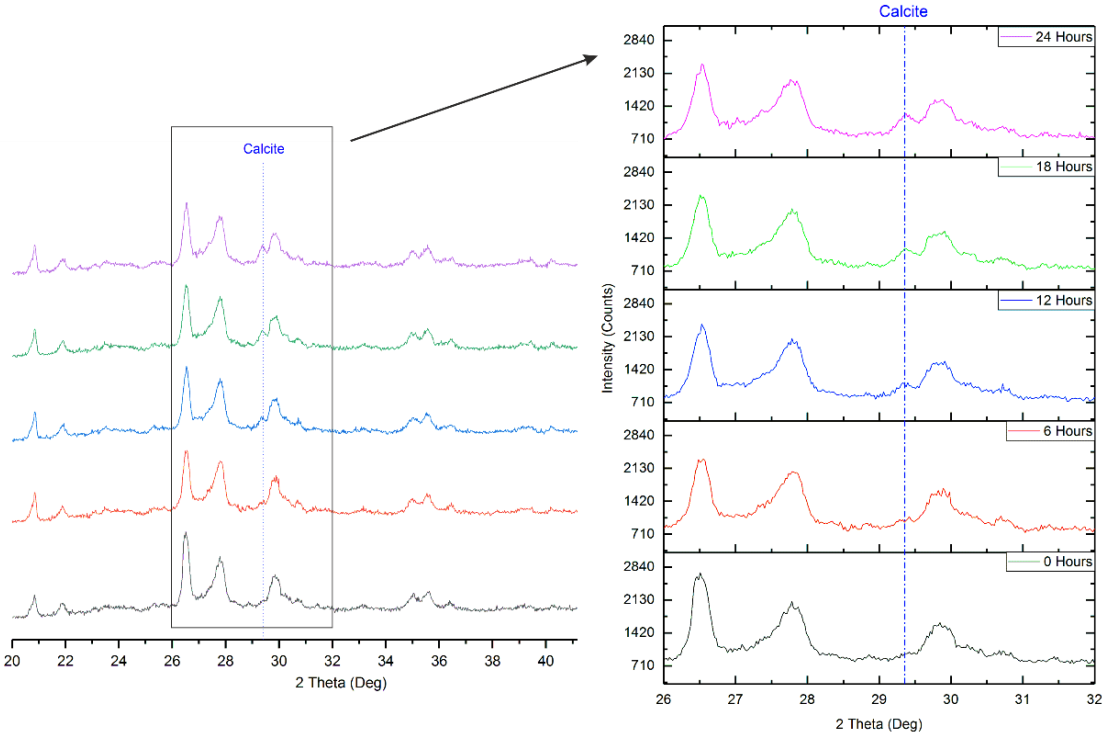

Figure 3. In situ XRD MPC2 pattern where d = 3.04 Å, reflection corresponding to precipitated newly formed calcite.

Therefore, the carbonation process occurred in the following two steps: a) silicate mineral dissolution and b) carbonate precipitation. Several studies based on the mineral carbonation of wollastonite [27,28] described the process in an aqueous carbonation route as:

1. Dissolution of CO_2 in water for the production of a (bi-)carbonate:

$$CO_2\ (g) + H_2O\ (l) \rightarrow H_2CO_3\ (aq) \rightarrow HCO_3^-\ (aq) + H^+\ (aq). \quad (5)$$

2. Leaching Ca from wollastonite by acidic attack:

$$CaSiO_3\ (s) + 2H^+\ (aq) \rightarrow Ca^{2+}\ (aq) + H_2O\ (l) + SiO_2\ (s). \quad (6)$$

3. Nucleation and growth of calcium carbonate:

$$Ca^{2+}\ (aq) + HCO_3^-\ (aq) \rightarrow CaCO_3\ (s) + H^+\ (aq). \quad (7)$$

These new carbonate crystals were observed by stereomicroscope (optical microscopy) and scanning electron microscopy (Figures 4 and 5), with a composition close to theoretical calcite, as shown by the results of elemental analysis by EDS.

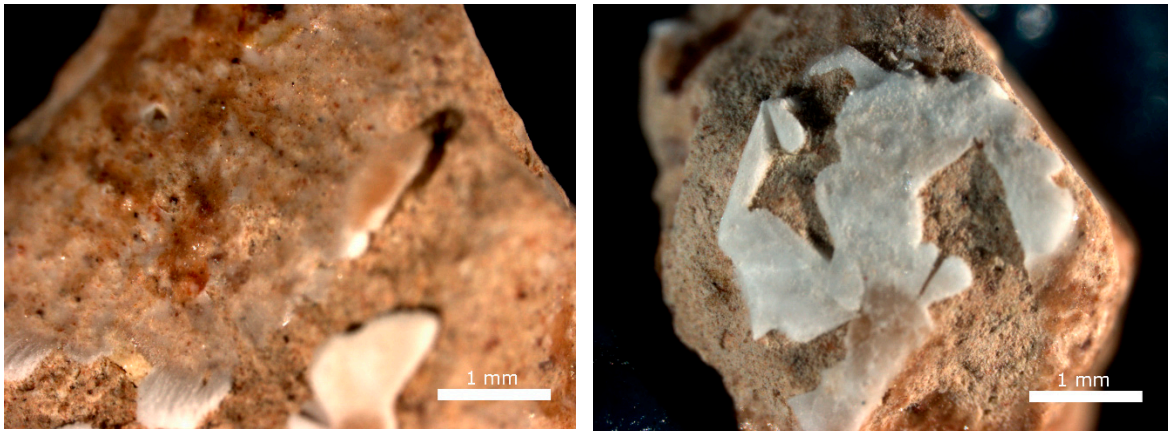

Figure 4. Layers of calcite on the MPC2 surface, observed by stereomicroscope after 720 h of CO_2 treatment.

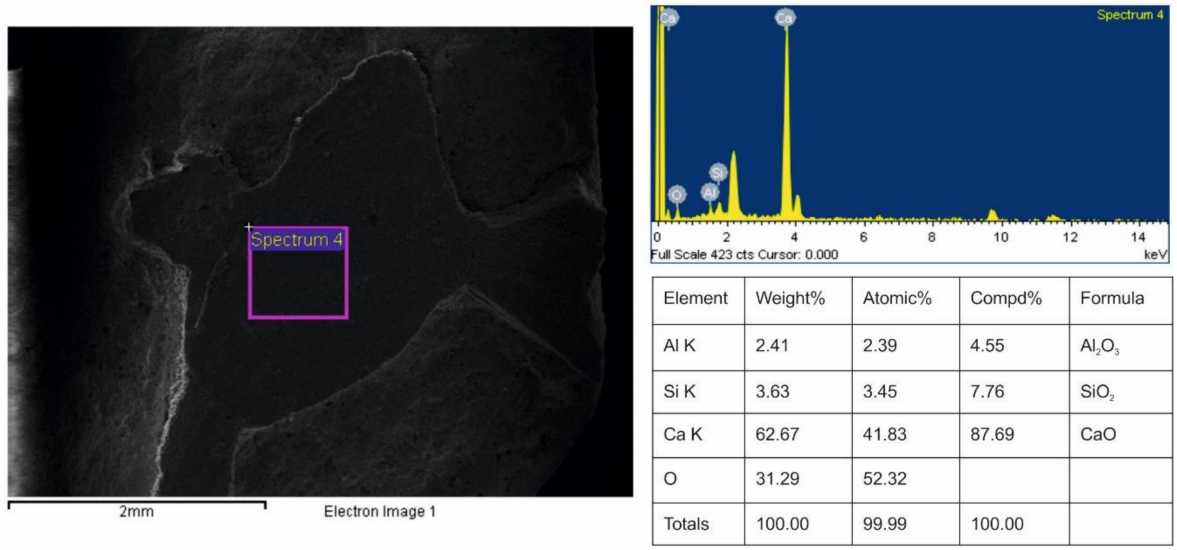

Element	Weight%	Atomic%	Compd%	Formula
Al K	2.41	2.39	4.55	Al_2O_3
Si K	3.63	3.45	7.76	SiO_2
Ca K	62.67	41.83	87.69	CaO
O	31.29	52.32		
Totals	100.00	99.99	100.00	

Figure 5. Scanning-electron-microscopy (SEM) image, and the energy-dispersive-spectrometer (EDS) spectrum and elemental quantification of MPC2.

The measurement of elemental carbon and weight loss by DTA-TG in the temperature range of the calcite decomposition (Table 3 or Figure 6a) was used to quantify the amount of captured CO_2. Both results could be expressed in terms of calcite as carbonate ore. Obviously, it was an indirect method due to it being assumed, on the one hand, that the only phase that decomposes in that temperature range was calcite and, on the other hand, that it only precipitates calcite as a carbonated material. This weight loss also corresponded to the expulsion of CO_2 and carbon content that was related to the theoretical content of CO_2 in the chemical composition of calcite (Equations (8) and (9)) [37,38].

$$\begin{aligned} \%\ \mathrm{Calcite}_{\mathrm{DTA-TG}} &= \frac{\Delta m_{450-900^{\circ}C}}{CO_2 \mathrm{Theorical}} \times 100 = \frac{\Delta m_{450-900^{\circ}C}}{43.97} \times 100 = 2.274 \times \\ \Delta m_{450-900^{\circ}C} \%\ \mathrm{Calcite}_{\mathrm{DTA-TG}} &= \frac{\Delta m_{450-900^{\circ}C}}{CO_2 \mathrm{Theorical}} \times 100 = \frac{\Delta m_{450-900^{\circ}C}}{43.97} \times 100 = 2.274 \times \Delta m_{450-900^{\circ}C} \end{aligned} \quad (8)$$

$$\%\ Calcite_{C-Elmental} = \frac{C_{content}}{C_{Theorical}} \times 100 = \frac{C_{content}}{12} \times 100 = \frac{25}{3} C_{content} \quad (9)$$

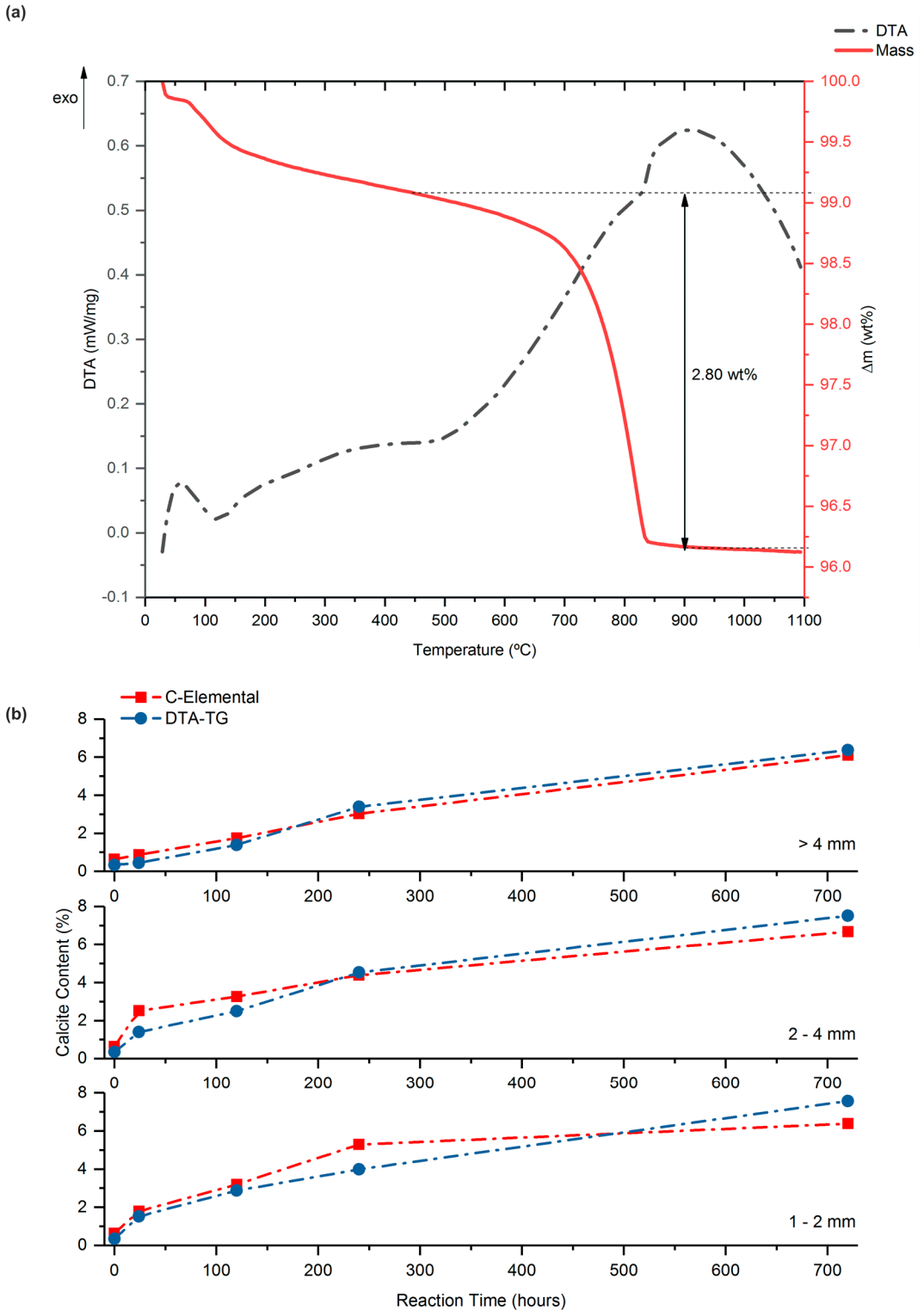

Figure 6. (**a**) MPC2 thermogravimetry (solid line) and differential thermal analyses (dashed line); >4 mm and 720 h reaction time. (**b**) Calculated calcite content by DTA-TG (circle) and by C element (square) as function of reaction time and particle size fraction (modified from [5]).

Table 3. Carbon elemental content, mass loss by differential thermal and thermogravimetric analysis (DTA-TG), and calcite content calculated by both techniques.

Particle Size	Reaction Time	C-Elemental	Mass Loss	Calcite	Calcite
(mm) MPC2	(hours)	(wt %)	(wt %)	(wt %) by C-Elemental	(wt %) by DTA-TG
Original	0	0.08	0.15	0.63	0.34
>4 mm	24	0.10	0.20	0.87	0.45
>4 mm	120	0.21	0.61	1.74	1.39
>4 mm	240	0.36	1.49	3.02	3.39
>4 mm	720	0.73	2.80	6.10	6.37
2–4 mm	24	0.30	0.61	2.51	1.39
2–4 mm	120	0.39	1.10	3.26	2.50
2–4 mm	240	0.53	1.99	4.38	4.53
2–4 mm	720	0.80	3.30	6.67	7.51
1–2 mm	24	0.21	0.67	1.79	1.52
1–2 mm	120	0.38	1.26	3.19	2.87
1–2 mm	240	0.63	1.75	5.29	3.98
1–2 mm	720	0.77	3.33	6.38	7.57

The difference compared to carbon analysis using the elemental analyzer could be attributed to the sum of experiment errors and analysis sensitivity. Yet, it was also necessary to take account of the adsorbed CO_2, which could be measured in CHNS instead of DTA. However, both followed the same tendency with respect to reaction times (Figure 6b). In both instances, calcite content was higher than the original and directly proportional to the reaction time in the studied size fractions.

The wollastonite attack with carbonic acid allowed for the release of calcium ions and calcite precipitation. Concerning the presence of soluble ions (Figure 7 and Table S4 in Supplementary Materials), the amount of Ca ions decreased over reaction time because of calcite precipitation, while Si increased as a consequence of partial silicate destruction. This partial destruction of silicates resulted in a new specific surface on the bulk (Figure 8). The increase of the specific surface had a direct relationship reaction time. The newly precipitated calcite on the sample surface also increased BET. However, both possibilities must have had a greater effect than physical CO_2 absorption that would result in a reduction of the specific surface area.

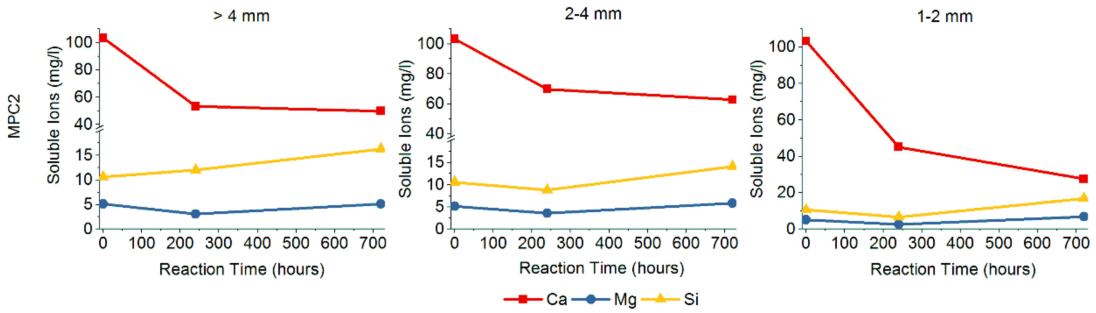

Figure 7. Soluble Ca, Mg, and Si ions measured untreated and treated after 240 and 720 h of reaction for MPC2 (modified from [5]).

After the carbonation tests, the brick samples revealed macro- and mesoporosity as determined by Hg porosity, which affects the proportion and size of the pores (Figure 9a,b), with a decrease in microporosity and increase in nanoporosity by N_2 and CO_2 absorption (Figure 9c,d). All of them were a result of two differentiated processes: (a) the action of carbonic acid destroying calcium silicates that produced an irregular surface and an increment of macro- and mesoporosity, and (b) the precipitation of carbonates that filled the micropores and probably reduced them to nanopores.

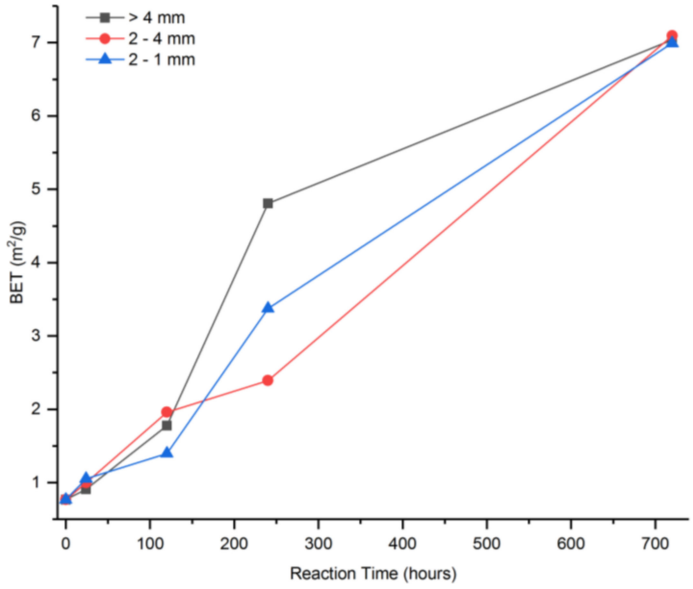

Figure 8. Specific surface evolution by specific surface area (BET) as a function of reaction time for MPC2 (modified from [5]).

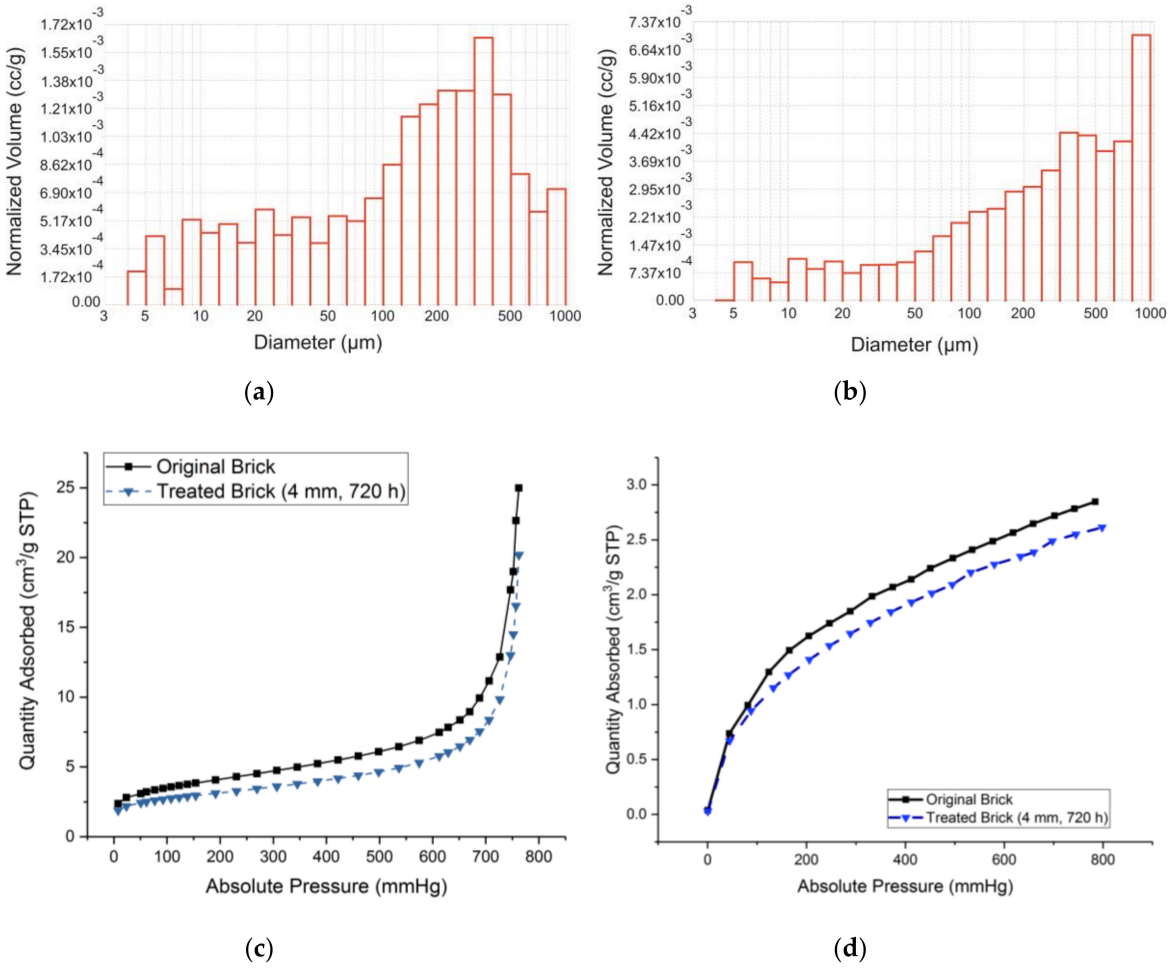

Figure 9. (**a**,**b**) Histograms of Hg porosity, (**c**) N_2 adsorption, and (**d**) CO_2 adsorption isotherms for original brick and treated brick layer.

Calculating efficiency was as the quotient between the percentage of captured CO_2 (experimental) and theoretical CO_2 by Steinour's formulae (Equation (4); Table 4). The calculated capture efficiency was proportional to the reaction time (the longer the time was, the higher the carbonation amount), whereas carbonation did not seem to significantly depend on particle size in the studied conditions. Results obtained at low pressure (1 bar) after 720 h of reactions for the total sample were very similar to those obtained for the finer fractions (2–4, 1–2 mm) at 10 bars.

Table 4. Carbonation efficiency (CE) according to Steinour's equation.

Particle Size (mm) MPC2	Pressure (bar)	Reaction Time (hours)	CO_2 Exp (wt %)	Efficiency (%)
Original	10	0	0.15	1.00
>4 mm	10	24	0.20	1.32
>4 mm	10	120	0.61	4.08
>4 mm	10	240	1.49	9.94
>4 mm	10	720	2.80	18.67
2–4 mm	10	24	0.61	4.08
2–4 mm	10	120	1.10	7.33
2–4 mm	10	240	1.99	13.28
2–4 mm	10	720	3.30	22.02
1–2 mm	10	24	0.67	4.46
1–2 mm	10	120	1.26	8.41
1–2 mm	10	240	1.75	11.67
1–2 mm	10	720	3.33	22.19
Total Fraction	1	720	3.20	21.33

4. Conclusions

The present research showed a suitable methodology to evaluate the possibility of using ceramic construction waste (or other types of construction and demolition waste) for mineral carbonation under surface conditions in short periods of time. Even though the experiment was conducted in comparatively large scale, each test method yielded only a very small fraction. Therefore, to increase reliability each test could be conducted several times.

Specifically, Ca-rich bricks were successfully used as raw material for direct mineral carbonation by the destruction of Ca silicates. The amount of carbonation was proportional to the reaction time, whereas it did not seem to significantly depend on particle size or pressure in the studied conditions.

Acceptable carbonation efficiency was achieved under the favorable conditions of low pressure and temperature.

These results open the possibility for future studies using the proposed methodology for other types of construction and demolition waste rich in calcium silicates or other calcium compounds, which could be directly carbonated by in situ injections of CO_2.

Supplementary Materials: The following are available online at http://www.mdpi.com/2075-163X/9/10/612/s1, Table S1: List of certificated standars used for XRF calibration.; Table S2: Detection limit (L.D.), quantification limit (L.C.) and relative error for the measuremento of the mayor elements by XRF in Panalytical Axios spectrometer of the SGI Laboratorio de Rayos X (University of Seville) [September 2014]; Table S3: Mayor elements comparative between monitor standards (calibration validation) in white box and the certificate value in grey box [September 2014]; Table S4: Soluble Ca, Mg, and Si ions measured untreated and treated after 240 and 720 h of reaction for MPC2 and their standard deviations.

Author Contributions: D.M. collected and analyzed the data and wrote the paper; V.F.-A. conceived and designed the ideas; and revised the paper; P.A. made the formal Investigation, discuss the data and revised/edited the manuscript.

Funding: This research was funded by the Junta de Andalucía (Consejería de Economía y Conocimiento) (P12-RNM-568 MO project) and the contract of Domingo Martín granted by the V Plan Propio de Investigación de la Universidad de Sevilla.

Acknowledgments: Authors are grateful to editor and reviewers for their comments which improved the manuscript. XRD, XRF, ICP-OES, C-elemental and SEM analysis were performed using the facilities of the General Research Center at the University of Seville (CITIUS).

Conflicts of Interest: The authors declare no conflict of interest.

References

1. Alberola, E.; Chevallier, J.; Chèze, B. The EU emissions trading scheme: The effects of industrial production and CO_2 emissions on carbon prices. *Econ. Int.* **2008**, *4*, 93–125. [CrossRef]
2. Caldeira, K.; Jain, A.K.; Hoffert, M.I. Climate sensitivity uncertainty and the need for energy without CO_2 emission. *Science* **2003**, *299*, 2052–2054. [CrossRef] [PubMed]
3. Pan, S.-Y.Y.; Chang, E.E.; Chiang, P.C. CO_2 capture by accelerated carbonation of alkaline wastes: A review on its principles and applications. *Aerosol Air Qual. Res.* **2012**, *12*, 770–791. [CrossRef]
4. Martín, D.; Aparicio, P.; Galán, E. Mineral carbonation of ceramic brick at low pressure and room temperature. A simulation study for a superficial CO_2 store using a common clay as sealing material. *Appl. Clay Sci.* **2018**, *161*, 119–126. [CrossRef]
5. Martín, D.; Aparicio, P.; Galán, E. Accelerated Carbonation of Ceramic Materials. Application to Bricks from Andalusian Factories (Spain). *Constr. Build. Mater.* **2018**, *181*, 598–608. [CrossRef]
6. Martín, D.; Aparicio, P.; Galán, E. Time evolution of the mineral carbonation of ceramic bricks in a simulated pilot plant using a common clay as sealing material at superficial conditions. *Appl. Clay Sci.* **2019**, *180*, 105191. [CrossRef]
7. Eighmy, T.; Gardner, K.; Seager, T. Method for Sequestering Carbon Dioxide. U.S. Patent US20050238563A1, 27 October 2005. Available online: https://patentimages.storage.googleapis.com/bb/49/8c/56d81ea0f8406a/US20050238563A1.pdf (accessed on 3 October 2019).
8. Montes-Hernandez, G.; Pérez-López, R.; Renard, F.; Charlet, L.; Nieto, J.-M. Process for Sequestration of CO2 by Reaction with Alkaline Solid Waste. European Patent EP 07 1233005.5, 14 December 2007. Available online: https://patentimages.storage.googleapis.com/47/a0/49/787d3e0e245078/WO2007071633A1.pdf (accessed on 3 October 2019).
9. Mayoral, M.C.; Andrés, J.M.; Gimeno, M.P. Optimization of mineral carbonation process for CO_2 sequestration by lime-rich coal ashes. *Fuel* **2013**, *106*, 448–454. [CrossRef]
10. Santos, R.M.; Van Bouwel, J.; Vandevelde, E.; Mertens, G.; Elsen, J.; Van Gerven, T. Accelerated mineral carbonation of stainless steel slags for CO_2 storage and waste valorization: Effect of process parameters on geochemical properties. *Int. J. Greenh. Gas Control* **2013**, *17*, 32–45. [CrossRef]
11. Sipilä, J.; Teir, S.; Zevenhoven, R. Carbon Dioxide Sequestration by Mineral Carbonation Literature Review Update 2005–2007. Report VT 2008-1. p. 52. Available online: http://innovationconcepts.nl/res/literatuurGPV/mineralcarbonationliteraturereview0507.pdf (accessed on 3 October 2019).
12. Soong, Y.; Fauth, D.L.; Howard, B.H.; Jones, J.R.; Harrison, D.K.; Goodman, A.L.; Gray, M.L.; Frommell, E.A. CO_2 sequestration with brine solution and fly ashes. *Energy Convers. Manag.* **2006**, *47*, 1676–1685. [CrossRef]
13. Uibua, M.; Kuusik, R.; Andreas, L.; Kirsimäe, K. The CO_2-binding by Ca-Mg-silicates in direct aqueous carbonation of oil shale ash and steel slag. *Energy Procedia* **2011**, *4*, 925–932. [CrossRef]
14. Gunning, P.J.; Hills, C.D.; Carey, P.J. Accelerated carbonation treatment of industrial wastes. *Waste Manag.* **2010**, *30*, 1081–1090. [CrossRef] [PubMed]
15. Geerlings, J.J.C.; Van Mossel, G.A.F.; Veen, B.C.M.I. Process for Sequestration of Carbon Dioxide by Mineral Carbonation. U.S. Patent US20100196235A1, 25 May 2010. Available online: https://patentimages.storage.googleapis.com/47/b3/78/16189676247184/US20100196235A1.pdf (accessed on 3 October 2019).
16. Kawatra, S.K.; Eisele, T.C.; Simmons, J.J. Capture and Sequestration of Carbon Dioxide in Flue Gases. U.S. Patent 7.919.064B2, 5 April 2011. Available online: https://patentimages.storage.googleapis.com/3d/6c/86/beea6a2fc7f1ba/US7919064.pdf (accessed on 3 October 2019).

17. Riman, R.E.; Atakan, V. Systems and Methods for Carbon Capture and Sequestration and Compositions Derived Therefrom. U.S. Patent US8114367B2, 14 February 2012. Available online: https://patentimages.storage.googleapis.com/72/67/38/c293969a42ecee/US8114367.pdf (accessed on 3 October 2019).
18. Galán, E.; Aparicio, P. Captura y Secuestro de CO2 Mediante la Carbonatición de Residuos Cerámicos. WITO Patent WO2011089292A1, 28 July 2011.
19. Costa, G.; Baciocchi, R.; Polettini, A.; Pomi, R.; Hills, C.D.; Carey, P.J. Current status and perspectives of accelerated carbonation processes on municipal waste combustion residues. *Environ. Monit. Assess.* **2007**, *135*, 55–75. [CrossRef] [PubMed]
20. Dri, M.; Sanna, A.; Maroto-Valer, M.M. Mineral carbonation from metal wastes: Effect of solid to liquid ratio on the efficiency and characterization of carbonated products. *Appl. Energy* **2014**. [CrossRef]
21. Huntzinger, D.N.; Gierke, J.S.; Sutter, L.L.; Kawatra, S.K.; Eisele, T.C. Mineral carbonation for carbon sequestration in cement kiln dust from waste piles. *J. Hazard. Mater.* **2009**, *168*, 31–37. [CrossRef]
22. Li, X.; Bertos, M.F.; Hills, C.D.; Carey, P.J.; Simon, S. Accelerated carbonation of municipal solid waste incineration fly ashes. *Waste Manag.* **2007**, *27*, 1200–1206. [CrossRef]
23. Haselbach, L. Potential for carbon dioxide absorption in concrete. *J. Environ. Eng.* **2009**, *135*, 465–472. [CrossRef]
24. Fernández Bertos, M.; Simons, S.J.R.; Hills, C.D.; Carey, P.J. A review of accelerated carbonation technology in the treatment of cement-based materials and sequestration of CO_2. *J. Hazard. Mater.* **2004**, *112*, 193–205. [CrossRef]
25. Seifritz, W. CO_2 disposal by means of silicates. *Nature* **1990**, *345*, 486. [CrossRef]
26. Lackner, K.S.; Wendt, C.H.; Butt, D.P.; Joyce, E.L.; Sharp, D.H. Carbon dioxide disposal in carbonate minerals. *Energy* **1995**, *20*, 1153–1170. [CrossRef]
27. Huijgen, W.J.J.; Witkamp, G.J.; Comans, R.N.J. Mechanisms of aqueous wollastonite carbonation as a possible CO_2 sequestration process. *Chem. Eng. Sci.* **2006**, *61*, 4242–4251. [CrossRef]
28. Daval, D.; Martinez, I.; Corvisier, J.; Findling, N.; Goffé, B.; Guyot, F. Carbonation of Ca-bearing silicates, the case of wollastonite: Experimental investigations and kinetic modeling. *Chem. Geol.* **2009**, *262*, 262–277. [CrossRef]
29. Huijgen, W.J.J.; Ruijg, G.J.; Comans, R.N.J.; Witkamp, G.J. Energy consumption and net CO_2 sequestration of aqueous mineral carbonation. *Ind. Eng. Chem. Res.* **2006**, *45*, 9184–9194. [CrossRef]
30. Tai, C.Y.; Chen, W.; Shih, S. Factors affecting wollastonite carbonation under CO_2 supercritical conditions. *AIChE J.* **2006**, *52*, 292–299. [CrossRef]
31. Huntzinger, D.N.; Gierke, J.S.; Kawatra, S.K.; Eisele, T.C.; Sutter, L.L. Carbon Dioxide Sequestration in Cement Kiln Dust through Mineral Carbonation. *Environ. Sci. Technol.* **2009**, *43*, 1986–1992. [CrossRef] [PubMed]
32. Steinour, H.H. Some effects of carbon dioxide on mortars and concrete-discussion. *J. Am. Concr. Inst* **1959**, *30*, 905–907.
33. Yixin, S.; Xudong, Z.; Monkman, S. A new CO_2 sequestration process via concrete products production. In Proceedings of the 2006 IEEE EIC Climate Change Conference, Ottawa, ON, Canada, 10–12 May 2006.
34. Wang, W.; Xiao, J.; Wei, X.; Ding, J.; Wang, X.; Song, C. Development of a new clay supported polyethylenimine composite for CO_2 capture. *Appl. Energy* **2014**, *113*, 334–341. [CrossRef]
35. Mun, M.; Cho, H. Mineral carbonation for carbon sequestration with industrial waste. *Energy Procedia* **2013**, *37*, 6999–7005. [CrossRef]
36. Prigiobbe, V.; Hänchen, M.; Werner, M.; Baciocchi, R.; Mazzotti, M. Mineral carbonation process for CO_2 sequestration. *Energy Procedia* **2009**, *1*, 4885–4890. [CrossRef]
37. Lim, M.; Han, G.C.; Ahn, J.W.; You, K.S. Environmental remediation and conversion of carbon dioxide (CO_2) into useful green products by accelerated carbonation technology. *Int. J. Environ. Res. Public Health* **2010**, *7*, 203–228. [CrossRef]
38. Villagrán-Zaccardi, Y.A.; Egüez-Alava, H.; De Buysser, K.; Gruyaert, E.; De Belie, N. Calibrated quantitative thermogravimetric analysis for the determination of portlandite and calcite content in hydrated cementitious systems. *Mater. Struct.* **2017**, *50*, 179. [CrossRef]